Effects of Pressure on the Chemical Properties of Solid Surface. VI. The Surface Acidity of the Compressed Zinc Sulfate

Takeshi KAWAKAMI, Akira USUI, and Yoshisada OGINO
Department of Chemical Engineering, Faculty of Engineering, Tohoku University, Aoba, Aramaki, Sendai

(Received June 24, 1971)

In order to clarify the mechanism of the acidity change due to compression, zinc sulfate was compressed under various pressures, ranging from 0 to 7000 kg/cm^2, and the surface acidity was measured and compared with the data of the structural change in the sample. According to the experimental results, the surface acidity varied on compression. At lower compacting pressures ($P \sim 2500$ kg/cm^2), the content of weak acid (H_0=1.5—3.3) was high and that of the strong acid was poor. These facts were explained by the higher content of anion-water, or heptahydrate, in the sample. In the pressure region of P=2500<5500 kg/cm^2, the acidity-pressure curve showed a maximum at 4500 kg/cm^2. Further, in this pressure range, the acidity-pressure curve paralleled well the respective curves of the X-ray peak width of hexahydrate pressure, the relative intensity of the IR $\nu_1(SO_4^{2-})$-pressure, and the half width of the IR $\nu_3(SO_4^{2-})$-pressure. It was considered that the acidity change in this pressure range is caused by the change in the content of the distorted structural unit of hexahydrate in the sample. In the highest pressure range, the content of weak acid was found to increase, whereas the content of strong acid was found to decrease. These results were discussed by considering the increased inclusion of tetrahydrate in the sample.

It has been revealed by the earlier works of the present authors[1-3] that the surface acidity of a solid varies on compression, and in the immediately preceding work[4] the authors have attemped to clarify the mechanism of the acidity change in aluminum sulfate. It has been demonstrated that the acidity change can be explained in terms of a microscopic structural change of the sample.

The purpose of the present work is to investigate whether or not the same mechanism as for the acidity change in aluminum sulfate is applicable to the acidity change in zinc sulfate. The details of the experimental results, including the acidity change, as well as the structural change in the sample will be described in this paper. Further, the validity of the previously-proposed mechanism of the acidity change will be demonstrated in the discussion.

Experimental

Material. The zinc sulfate heptahydrate was purified by means of recrystallization, and the resulting sulfate was used as the raw material for the sample.

Preparation of the Compressed Sample. The raw sulfate was compressed by the procedures described in the previous papers.[1-4] Briefly, the compression was carried out over a 10 min period under various pressures, ranging from 0 to 7000 kg/cm^2 and at a temperature of 20°C. The resulting cylindrical pellet, 6 mm in diameter and 2 mm in height, was pulverized in a mortar, and the powdered material was subjected to drying in a vacuum for 45 min at a temperature of 18°C. Then the powder served as a sample for the desired measurement. In order to minimize the effects of the change in ambient conditions, the following operations, *i.e.*, compressions, pulverizings, dryings, and weighings, were carried out in an air-conditioned room.

For the sake of convenience, the respective samples which were compressed under 0, 2500, 4500, 5500, and 7000 kg/cm^2 were defined as P_0, P_{2500}, P_{4500}, P_{5500}, and P_{7000}.

Surface Acidity. The surface acidity was determined by Benesi's method[5] with the following four indicators: dicinnamalacetone (pK_a=−3.0), crystal violet (pK_a=0.8), benzeneazodiphenylanmie (pK_a=1.5), and *p*-diphenylaminoazobenzene (pK_a=3.3). The acidity measurements were also carried out in an air-conditioned room.

Qualitative Tests for Lewis Acid. The identification of the Lewis acid center on the sample surface was carried out by the procedures used in a previous work.[4]

Surface Areas. The specific surface area of the sample evaluated by applying the BET thory to the adsorption data of nitrogen at −195°C.

Differential Thermal Analysis(DTA) and Thermogravimetric Analysis(TGA). DTA and TGA runs were carried out on a Rigaku Denki unit. The DTA curves and TGA curves were obtained at a temperature programming rate of 5°C/min.

X-Ray Diffraction. Powder X-ray diffraction patterns of the sample were obtained with a Shimadzu GX-1 X-ray Diffractometer. The Cu$K\alpha$ radiation (Ni filter) at 30 KV and 15 mA was used.

Infrared Spectroscopy. The infrared spectra for a 400~4000 cm^{-1} wave number range were obtained with a Perkin-Elmer Model 125 Infrared Spectrophotometer. In this work, a Nujol technique was employed.

Results

Surface Acidity. In Fig. 1, the acidity values of a given H_0 value are plotted against the compacting pressure. As can be seen in this figure, the acidity of H_0=−3.0~0.8 and the acidity of H_0=0.8~1.5 both increase with an increase in the compacting pressure and reach a maximum at a compacting pressure of 4500 kg/cm^2; a further increase in the compacting pressure results in a decrease in the surface acidity. On the other hand, the pressure dependence of the content of weak acid (H_0=1.5~3.3) showed a com-

---

[1] Y. Ogino and T. Kawakami, This Bulletin, **38**, 972 (1965).

[2] Y. Ogino, T. Kawakami, and K. Tsurumi, *ibid.*, **39**, 639 (1966).

[3] Y. Ogino, T. Kawakami, and T. Matsuoka, *ibid.*, **39**, 859 (1966).

[4] T. Kawakami, A. Konno, and Y. Ogino, *ibid.*, **44**, 1772 (1971).

[5] H. A. Benesi, *J. Phys. Chem.*, **61**, 970 (1957).

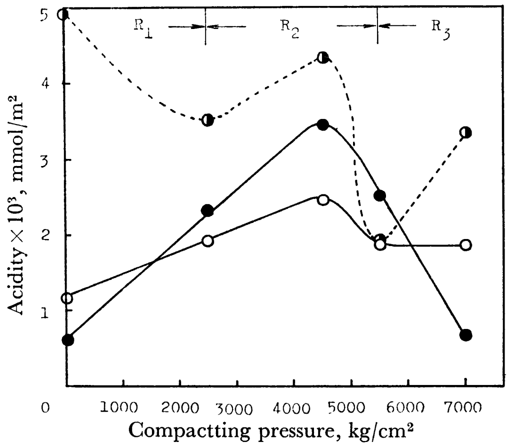

Fig. 1. Relations between the compacting pressure and the surface acidity: -○- $H_0=-3.0\sim0.8$, -●- $H_0=0.8\sim1.5$, -◐- $H_0=1.5\sim3.3$.

plicated behavior. Further, none of the samples showed any sign positive to the existence of Lewis acid.

Water Content. The water contents in samples compressed under various pressures are given in Table 1.

TABLE 1. WATER CONTENTS OF THE SAMPLES COMPRESSED UNDER VARIOUS PRESSURES

Compacting Pressure (kg/cm²)	0	2500	4500	5500	7000
Water Content (mol-H_2O/mol-$ZnSO_4$)	6.33	6.13	6.11	6.12	6.16

DTA and TGA. The DTA curves for various samples are given in Fig. 2. As can be seen in this figure, dehydration from the compressed sample occurred at 50, 98, and 240°C, while the dehydration from the uncompressed sample occurred at various temperatures. The TGA experiment and the chemical analysis gave the corresponding amounts of dehydration at 50 and 98°C. The results are summarized in Table 2. The data given in this table show that the endothermic DTA peak appearing at 50°C for the compressed samples may be attributed to the dehydration;

$$ZnSO_4 \cdot 6H_2O \longrightarrow ZnSO_4 \cdot 4H_2O + 2H_2O$$

and that the peak appearing at 98°C may be attributed to the dehydration;

$$ZnSO_4 \cdot 4H_2O \longrightarrow ZnSO_4 \cdot H_2O + 3H_2O$$

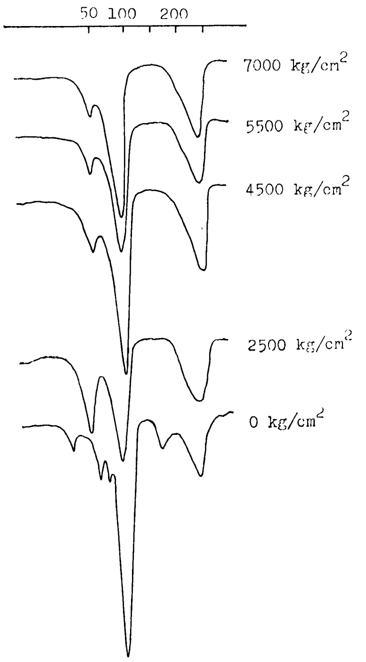

Fig. 2. D.T.A. curves for the samples compressed at various pressures.

TABLE 2. AMOUNT OF DEHYDRATION AT 50°C AND 98°C

Samples	50°C	98°C
P_{2500}	1.7 mol-H_2O/mol-$ZnSO_4$	3.6 mol-H_2O/mol-$ZnSO_4$
P_{4500}	1.9 mol-H_2O/mol-$ZnSO_4$	3.2 mol-H_2O/mol-$ZnSO_4$
P_{5500}	1.9 mol-H_2O/mol-$ZnSO_4$	3.3 mol-H_2O/mol-$ZnSO_4$
P_{7000}	2.0 mol-H_2O/mol-$ZnSO_4$	3.3 mol-H_2O/mol-$ZnSO_4$

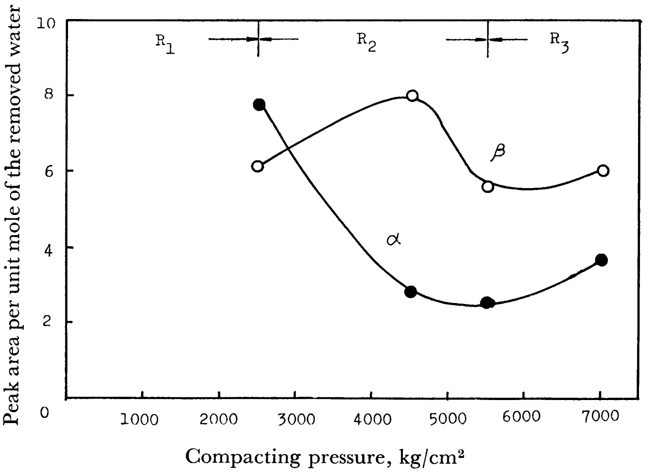

Fig. 3. Relations between the compacting pressure and the area of the endothermic peaks appeared at 50°C (-●-) and at 98°C (-○-).

The value of the endothermic DTA peak area per unit mole of removed water is given in Fig. 3. The area of the peak appearing at 50°C varied on compression and reached a minimum at a compacting pressure of 4500∼5500 kg/cm². On the contrary, the area of the peak appearing at 98°C increased with an increase in the compacting pressure and reached a maximum at a compacting pressure of 4500 kg/cm². A further increase in the compacting pressure resulted in a decrease in this peak area.

As can be seen in Fig. 2, there is a marked difference between the DTA curve of the uncompressed sample and that of the compressed sample. The DTA curve for the former sample has many more endothermic peaks than the DTA curve for the latter sample. This means that the uncompressed sample contains many kinds of crystallization water. As can be seen in the next section, the compressed sample contains both zinc sulfate heptahydrate and zinc sulfate hexahydrate, whereas the compressed sample contains mainly hexahydrate. (The possibility of the coexistence of a small amount of heptahydrate can not be excluded. Further, the coexistence of tetrahydrate $ZnSO_4 \cdot 4H_2O$ is also seen at pressures higher than 5500 kg/cm²). Thus,

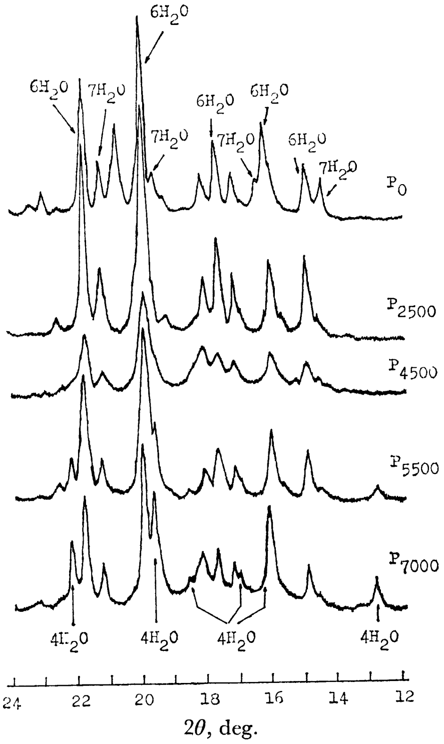

Fig. 4. X-ray diffraction patterns for various samples.

the complex DTA curve for the uncompressed sample may be attributed to the co-existence of hexahydrate and heptahydrate.

X-Ray Diffraction. Powder X-ray diffraction patterns for the various samples are igven in Fig. 4. From these patterns, it can be understood that the zinc sulfate used in this study consisted of crystals of heptahydrate[6] and hexahydrate.[7] Up to the compacting pressure of 4500 kg/cm^2, the line intensity of the heptahydrate decreased, and that of the hexahydrate increased, with an increase in the compacting pressure. However, this trend was reversed at compacting pressures higher than 4500 kg/cm^2.

Further, the degree of the broadening of the diffraction line for the hexahydrate increased with an increase in the compacting pressure from 0 to 4500 kg/cm^2, then it decreased at higher compacting pressures. In addition, diffraction peaks for tetrahydrate ($ZnSO_4 \cdot 4H_2O$) were found to appear (Fig. 4) in the diffraction pattern for the samples compressed at pressures higher than 5500 kg/cm^2.

Infrared Spectra. The infrared spectra for the sample compressed under various pressures are given in Fig. 5. Among the absorption bands in this figure, the bands assigned to ν_{OH} (3400 cm^{-1}), ν_{wag} (540 cm^{-1}),[8] and ν_{SO_2} (985 cm^{-1}) seemed to vary on compression. In view of the general difficulties in the comparison of the IR data for the polycrystalline hydrate, the following IR data are thought to include some ambiguities; they must be regarded as qualitative data even if they are expressed by numerical values (*e.g.*, the intensity or the relative intensity):

i) The shape of the absorption band appearing at 2800~3600 cm^{-1}, which was assigned to the OH stretching vibration, seemed to vary on compression,

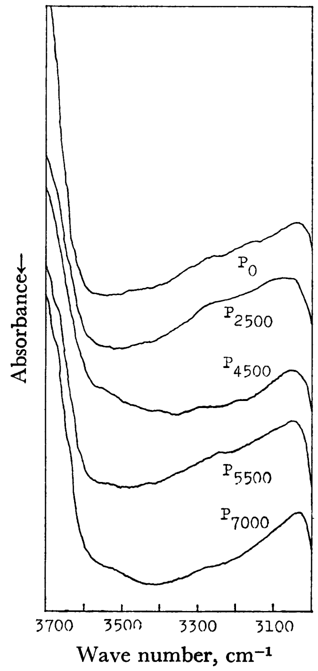

Fig. 5 A. Infrared spectra for various samples.

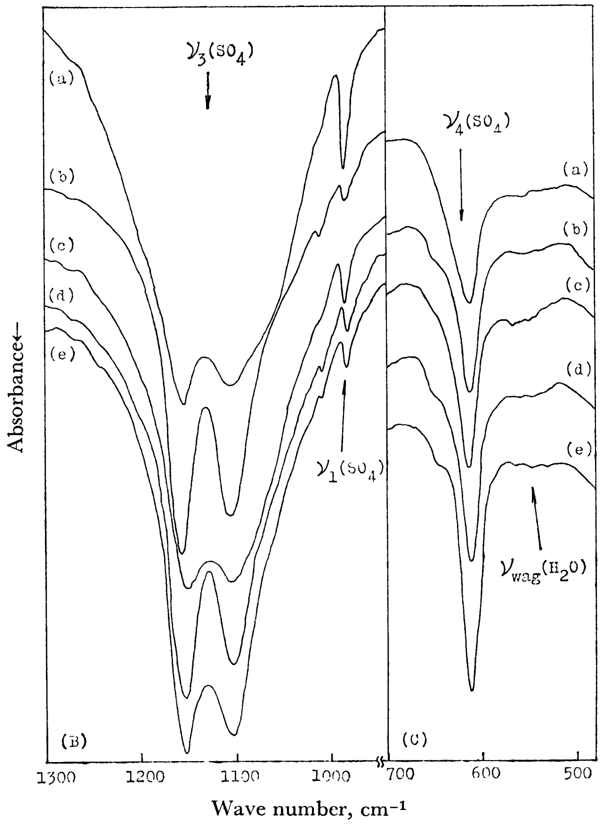

Fig. 5-B,C. Infrared spectra for the samples compressed at various pressures: (a) P_0; (b) P_{2500}; (c) P_{4500}; (d) P_{5500}; (e) P_{7000}.

---

[6] "Index to the Powder Diffraction Fill," ed. by J. V. Smith, ASTM Publications (1965), 9-395.

[7] *Ibid*, 1-0352.

[8] I. Nakagawa and T. Shimanouchi, *Spectrochimica Acta*, **20**, 429 (1964).

especially at 4500 kg/cm². From this fact, it was suspected that the absorption band for the P_{4500} sample shifted to somewhat lower wave numbers. However, this is only a suspicion. Because of the broad absorption band, the exact peak position could not be determined.

ii) The absorption appearing at 985 cm^{-1} was assigned to the ν_1 vibration of sulfate ions in the sample. The relative intensity[9] of this absorption against the intensity of the absorption for the ν_4 vibration of the sulfate ion (656 cm^{-1}) is given in Fig. 6. As can be seen in this figure, the relative intensity varied on compression.

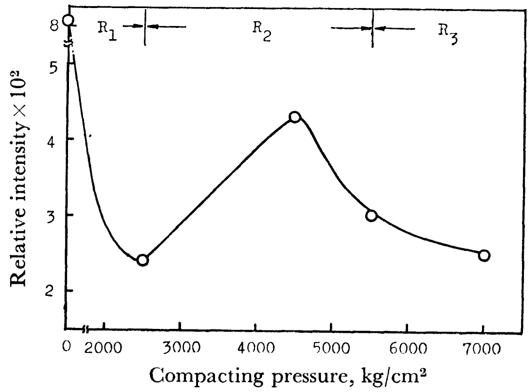

Fig. 6. Relations between the compacting pressure and the relative intensity of the ν_1 absorption against the ν_4 absorption for the sulfate ion.

iii) The absorption appearing at 540 cm^{-1} was assigned to the wagging vibration of the coordinated water in the sample. As can be seen in Fig. 5, the intensity[10] of this absorption seemed to increase with an increase in the compacting pressure, reaching a maximum at the compacting pressure of 4500 kg/cm², while it seemed to decrease at higher compacting pressures. Unfortunately, however, the reliability of this pressure-dependence for the H_2O wagging libration is not high enough because the absorption band at 540 cm^{-1} is broad and weak.

Discussion

Acidity Change on Compression and Related Data. Much as with the surface acidity of the other sulfates,[1-4] the surface acidity of zinc sulfate hydrate was found to vary on compression.

Generally speaking, the observed acidity change should be related to the structural change of the sample. However, as can be seen in Fig. 1, the surface acidity per unit surface area varied on compression. Therefore, the acidity change observed in the present study could not be attributed to the change in the surface area. Other factors must be related to the acidity change. It may be suspected that the dehydration from the sample might be directly causing the acidity change. However, efforts to correlate the acidity change with the degree of dehydration were not successful. It is difficult to derive any meaning from the small differences among the water contents of the various compressed samples (Table 1). In addition, approaches of this type seem to give little information about the microscopic cause of the acidity change.

In discussing the mechanism of the acidity change, the fact that the sample did not show any sign positive to Lewis acid must be taken into consideration. This fact and the experimental results given in Fig. 1 indicate that the acid which was found on the sample surface should be identified as Brönsted acid, which has a strength of $3.3 \geq H_0 \geq -3.0$. Therefore, the mechanism of the acidity change may be considered to include changes in the interaction among ions constituting the sample. From this point of view, the changes in the ionic arrangement in the sample must be compared with the acidity change.

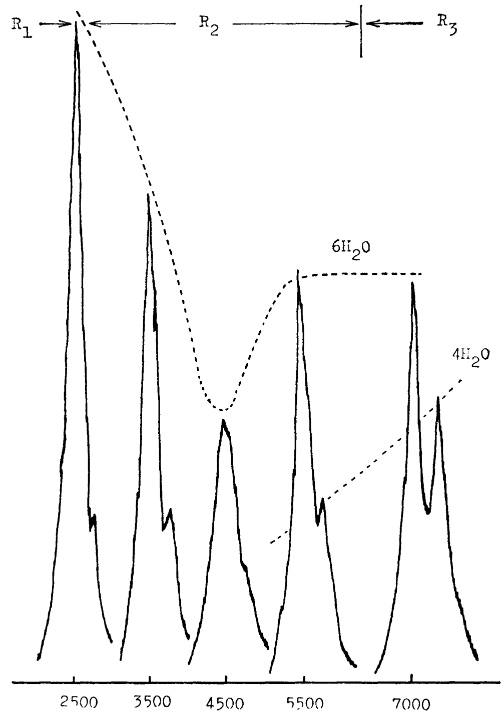

Fig. 7. Changes in the X-ray diffraction peak height ($2\theta=20.2°$).

On this point, information obtained from the X-ray diffraction study is useful. As can be seen in Fig. 7, the height of the X-ray diffraction peak at $2\theta=20.2°$, reached a minimum at the compacting pressure of 4500 kg/cm². Further, as can be seen in Fig. 8, the half-width of the diffraction peak reached its maximum at 4500 kg/cm². If these two figures are compared with Fig. 1, which shows the maximum acidity at 4500 kg/cm², an intimate relation between the acidity change and the change in the crystal structure becomes evident. However, the anomalously high acidities of $H_0=1.5\sim3.3$ for both samples of $P=0$ and $P=7000$ kg/cm² do not conform with the relation between the X-ray half-width ($2\theta=20.2°$) and the compacting pressure (Fig. 8). These facts seem to indicate that factors other than the change in the X-ray peak at $2\theta=20.2°$

---

[9] Defined by the ratio of the peak area.

[10] Defined by the peak area.

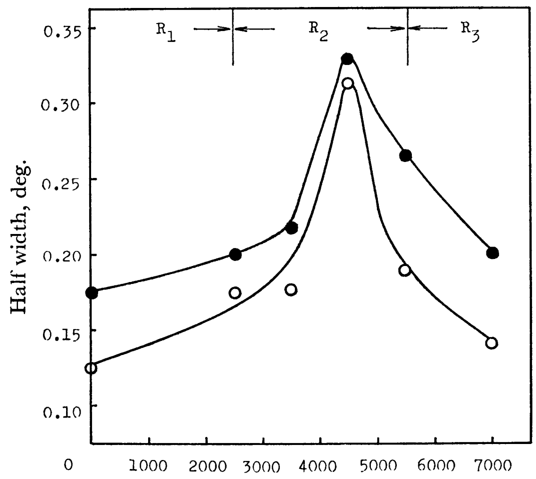

Fig. 8. Relations between the compacting pressure and the half-width of the X-ray diffraction peak for zinc sulfate hexahydrate: -●- $2\theta=20.2°$, -○- $2\theta=15.0°$.

(*i.e.*, the change in the crystal structure of hexahydrate) must be taken into consideration in order to discuss the acidities of the samples of $P=0$ and $P=7000$ kg/cm^2.

On the basis of the above discussion, the following discussion may be divided into three parts corresponding to three pressure regions-R_1, R_2, and R_3; R_1 ($P=0$ kg/cm^2) is a region where the anomalously high content of weak acid does not conform with the smaller half-width of the X-ray peak at $2\theta=20.2°$; R_2 ($P=2500\sim5500$ kg/cm^2) is a region where the acidity change conforms well with the change in the X-ray peak width, and R_3 ($P=5500$—7000 kg/cm^2) is a region where the existence of tetrahydrate becomes evident and the higher content of weak acid does not conform with the smaller X-ray half-width of hexahydrate ($2\theta=20.2°$).

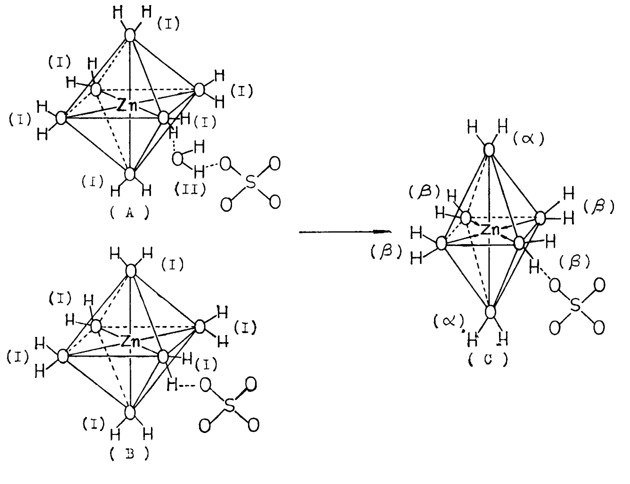

Fig. 9. Models of structural unit of zinc sulfate: (A) heptahydrate, (B) hexahydrate (not distorted), (C) hexahydrate (distorted).

Acidity Change and Structural Change in R_1. As can be seen in Fig. 1, the amount of weak acid ($H_0=1.5\sim3.3$) in the uncompressed sample was considerably great. On the other hand, the water content of this sample was also high compared with the other samples (Table 1). Further, the X-ray diffraction pattern for the uncompressed sample indicated rather strong peaks for heptahydrate. Therefore, it seems probable that the higher content of the weak acid in the uncompressed sample may be due to the higher content of anion-water (*cf.* Fig. 9-A) or to the presence of a heptahydrate.

In connection with the above discussion, it must be made clear that the relative intensity of the IR $\nu_1(SO_4^{2-})$ spectrum and the half-width of the $\nu_3(SO_4^{2-})$ spectrum were quite high for the uncompressed sample (Figs. 6, and 10). These facts may be ascribed to the higher content of anion-water. That is, it was considered that the anion-water may act to reduce the symmetry around sulfate ions in the sample.

The above view is rather crude, and more detailed discussions are desirable. Unfortunately, however, this is not possible at present. From a rather complicated feature appearing in the DTA chart for the uncompressed sample (Fig. 2), it is thought that the water molecules in this sample behave in a complex manner. Further, the easier dehydration observed at lower compacting pressures suggests that the uncompressed sample has an unstable structure. Thus, it is thought that the mechanism of the acidity change at compacting pressures lower than 2500 kg/cm^2 (in R_1) might be complex; more precise experimental work than the present experiments seem to be required to clarify the mechanism. For these reasons, detailed discussions of the acidity change in R_1 were not carried out in this paper.

One more point to be mentioned here is the low acidity for the strong acid ($H_0\leq1.5$) in this region (Fig. 1). Judging from the fact that the peak height for the X-ray diffraction of the uncompressed sample was generally high, both heptahydrate and hexahydrate seem to have their regular structural units. Therefore, there are few factors to strengthen the acid in the uncompressed sample. A higher content of anion-water may be an important factor in exhibiting the appearance of the strong acid. Thus, it may be possible to consider that the existence of heptahydrate is unfavorable for the appearance of strong acid.

Acidity Change and Structural Change in R_2.[11] As was mentioned in the previous section, the acidity change in this region was found to parallel well the change in the X-ray peak height or peak width for hexahydrate. Therefore, the acidity change in this region (R_2) may be related intimately to the change in the crystal structure of hexahydrate. Further, considering from the X-ray diffraction data (Fig. 4) and water content (Table 1), it may be estimated that the dominant species existing in the samples in the R_2 region are hexahydrate and that the existence of other species (heptahydrate and tetrahydrate) would have little effect on the acidity change because the contents of the latter species are considered to be small.

Under the provisions described above, the following discussions may be applicable to the acidity change in R_2. When changes in the crystal of hexahydrate occur, some changes in the structural unit constituting

---

[11] It must be noted that all the figure referred to in this part should be confined to the pressure region of 2500—5500 kg/cm^2.

the crystallite of hexahydrate may be expected to occur. Therefore, the intimate relation between the acidity change in R_2 and the change in the X-ray diffraction peak for hexahydrate seems to mean that the acidity change may be caused by the change in the structural unit of hexahydrate. This view is in accord with the results obtained in the preceding work.4) In order to aid the following discussions, models of the structural units of zinc sulfate hydrate,8) including the model of hexahydrate, are given in Fig. 9.

The structural unit of $ZnSO_4 \cdot 6H_2O$ contains 6 moles of the coordinated water. However, the DTA data shown in Fig. 2 indicate that the coordinated water in the compressed sample is not equivalent. Further, the TGA data showed that 2 moles of the coordinated water were removed by the heating at ~50°C, and that the remaining coordinated water was removed by heating at higher temperatures. Therefore, it may be plausible to consider that the compressed sample contains two sorts of coordinated water. Thus, the 2 mol of coordinated water which were removed at 50°C were defined as α, and the other coordinated water was defined as β. The 4 mol of β may be considered to consist of 3 mol of β_1 and 1 mol of β_2. The respective dehydration temperatures of β_1 and β_2 are 98 and 240°C. Unfortunately, however, it is not possible to decide which one of the four coordinated water specimen is β_2.

There are many reasons to consider that the interactions between the central Zn^{2+} ion and the coordinated water vary on compression. As can be seen in Fig. 3, the DTA endothermic peak area per unit of mole of the removed water varied on compressing the sample. The peak area for the dehydration of α-water decreased on compression and reached its minimum at the compacting pressure of 4500~5500 kg/cm². On the contrary; the peak area for the dehydration of β_1-water reached its maximum at 4500 kg/cm². These facts indicate that the interaction between Zn^{2+} and β_1 reached its maximum at 4500 kg/cm², while the interaction between Zn^{2+} and α reached its minimum in the vicinity of this compacting pressure.

As has been mentioned in the experimental section, the interpretation of the IR data for such polycrystalline hydrates as are used in the present work involves many difficulties. Therefore, the following discussions of the IR data should be regarded as crude and approximate. The purpose of the present discussion is to show that the results of the IR experiments exhibit qualitative parallelisms with the other experimental data, *i.e.*, the surface acidity, the X-ray diffraction, and the DTA.

As has been mentioned in connection with the experimental results, the IR absorption band at 3400 cm^{-1} (OH stretching) for the P_{4500} sample was suspected to shift toward lower wave numbers (Fig. 5A, P=2000~5500 kg/cm²). If this suspicion was not imaginary, the IR data in Fig. 5A (P=2000~5500 kg/cm²) would support the theory that the strongest interaction of Zn^{2+} with β occurred at P=4500 kg/cm². Further, the IR absorption for the H_2O wagging libration (540 cm^{-1}) seemed to be most intensified at P=4500 kg/cm² (Fig. 5C). Although the reliability of this spectral change was not high enough, the strongest interaction of Zn^{2+} with β at P=4500 kg/cm² seems to be suggested.

In addition to the above-mentioned changes in the infrared spectra for water, Fig. 5 shows that the infrared spectra for the sulfate ion varied also on compression. The changes in the half-widths of the ν_3 vibration of the sulfate ion and the relative intensity of the ν_1 vibration of the sulfate ion are given in Fig. 10 (P=2500~5500 kg/cm²). It can be seen that the largest change appeared at the compacting pressure of 4500 kg/cm². These facts seem to indicate that the interaction between the sulfate ion and its environments varied on compression. In view of the model of the structural unit, such changes as have been described above may be thought to occur easily. Presumably, the increased ν_1 absorption of SO_4^{2-}, which is originally inactive in the infrared absorption, may result from an increased interaction between the oxygen in the sulfate ion and the hydrogen in the coordinated water, β.

The acidity changes observed in the R_2 region seem to be explainable in terms of the structural unit of $ZnSO_4 \cdot 6H_2O$. The existence of two sorts of coordinated water, *i.e.*, α and β, means that the octahedron around the Zn^{2+} ion is distorted in the manner shown in Fig. 9-C (the distances between Zn^{2+} and H_2O (α) are extended and the distances between Zn^{2+} and H_2O (β) are shortened); moreover as has been mentioned in the previous section, the change in the interaction between the central Zn^{2+} and the coordinated water, β, may result from the change in the compacting pressure. The change in the interaction between Zn^{2+} and H_2O (β) may result in a change in the degree of the polarization of the H_2O (β) molecule in the following way:

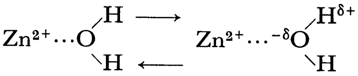

$$Zn^{2+}\cdots O\begin{smallmatrix}\diagup H \longrightarrow \\ \diagdown H \longleftarrow\end{smallmatrix} \qquad Zn^{2+}\cdots {}^{-\delta}O\begin{smallmatrix}\diagup H^{\delta+} \\ \diagdown H\end{smallmatrix}$$

Thus, the quantity of the protonic-acid center around the octahedral structural unit will vary. According to this mechanism, the acidity will become larger as the interaction between Zn^{2+} and H_2O (β) is increased.12)

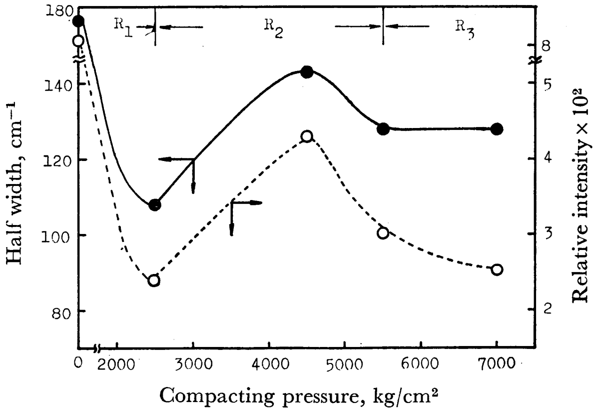

Fig. 10. Relations between the compacting pressure and the half width of the ν_3 absorption band of the sulfate ion (-○-), and the changes in the relative intensity of the ν_1 absorption against the ν_4 absorption for the sulfate ion (-●-).

---

12) G. Zundel, "Hydration and Intermolecular Interaction," Academic Press, New York (1969).

The parallelism between the acidity change (Fig.1) and the change in the dehydration peak area (Fig. 3) seems to indicate the validity of the above-mentioned mechanism for the acidity change. Further, the crude parallelism between the acidity change (Fig. 1) and the IR data for the OH stretching (Fig. 5A) and H_2O wagging libration (Fig. 5C) seems to be consistent with the proposed mechanism for the acidity change.

The interaction between the sulfate ion and the coordinated water (β) may also contribute to the acidity change. As has been mentioned in the previous section, the infrared spectra (Figs. 5 and 10) revealed that this interaction also varies on compression; the acidity change (Fig. 1) also paralleled the changes in the infrared spectra for the ν_1 and ν_3 vibrations of the sulfate ion (Fig. 10). Presumably, the compression resulted in a displacement of the sulfate ion nearer to the octahedral structural unit, and this promoted the polarization of the H_2O (β) molecule. Further support for this mechanism is given in Fig. 11. As can be seen in this figure, the relative intensity of the ν_1 absorption of SO_4^{2-} has a straight-line relationship to the acidity change.

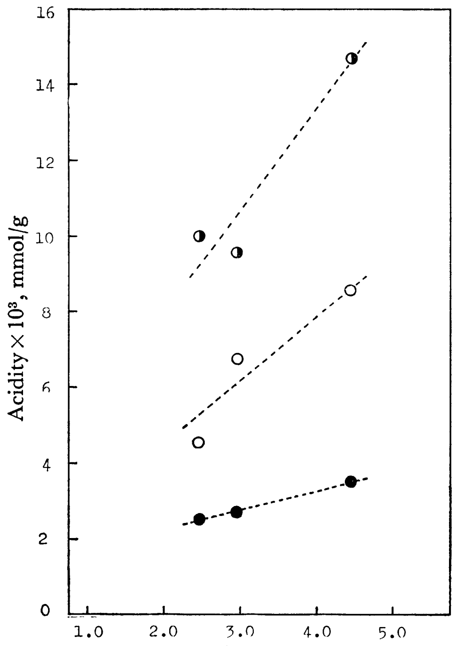

Fig. 11. Relations between surface acidity (H_0=−3.0∼0.8, -●-; H^0=−3.0∼1.5, -○-; H^0=−3.0∼3.3, -◑-) and the relative intensity of ν_1 absorption against the ν_4 absorption for the sulfate ion.

The pressure range of P=4500∼5500 kg/cm² seems to be a special region, though this pressure range was considered to belong to R_2. In this pressure range, the acidity was found to decrease despite the increasing pressure. As has been mentioned in the previous paragraphs, the decreasing acidity in R_2 is attributable to the decreasing distortion of the structural unit of hexahydrate. This decreasing distortion of the structural unit seems to be ascribable to the appearance of tetrahydrate. The X-ray diffraction data given in Fig. 4 show that the peak for tetrahydrate appears at 5500 kg/cm². It is probable that a part of the supplied energy of compression was consumed to produce tetrahydrate. Therefore, the energy to distort the structural unit may be reduced. Thus, the smaller content of the distorted structural unit and the smaller surface acidity may result. Of course, the formation of tetrahydrate would result in a decrease in the content of hexahydrate (probably accompanied by the formation of heptahydrate). However, judging from the rather weak diffraction peaks of tetrahydrate in R_2, other effects of tetrahydrate on the acidity change in R_2 may be considered to be small and negligible.

Acidity Change and Structural Change in R_3. As can be seen in Fig. 4, when the compacting pressure exceeds 5500 kg/cm² (especially at 7000 kg/cm²), the peaks for tetrahydrate ($ZnSO_4 \cdot 4H_2O$) became evident. On the other hand, the content of weak acid (H_0=1.5∼3.3, R_3 in Fig. 1) and the DTA peak area (β_1, R_3 in Fig. 3) increased in this region, R_3. Therefore, it is not unlikely that these changes are related directly to the existence of tetrahydrate. Unfortunately, however, direct evidence for this view is lacking at present. Whether the higher content of weak acid (H_0=1.5∼3.3) in the sample compressed at 7000 kg/cm² is due directly to the existence of tetrahydrate, or to the somewhat increased content of heptahydrate, is not certain. (Considering from the fairly constant water content in the compressed sample of $P \geq 2500$ kg/cm², the formation of tetrahydrate may proceed through a disproportionation of hexahydrate. Thus, the formation of tetrahydrate may accompany the formation of heptahydrate. According to the discussion in Part I, the existence of heptahydrate may be a cause of the appearance of weak acids.)

The behavior of the strong acid (H_0=−3.0∼1.5) in this region (R_3) is also interesting. In spite of the increase in the X-ray diffraction peaks for tetrahydrate, the acidity of $H_0 \leq 1.5$ tended to decrease beyond P=5500 kg/cm². Therefore, it may be said at least that the existence of tetrahydrate does not result in a marked increase in the content of strong acid. However, in view of the rather complicated structure and composition of the sample in this region (R_3), the possibility that the appearance of tetrahydrate might affect the acidity change (strong acid) in a complicated manner can not excluded.

One important role played by tetrahydrate in the acidity change (strong acid in R_3) seems to be the reduction of the compression energy which is available to distort the structural unit. In the pressure range where the appearance of tetrahydrate is more favorable, the energy of compression may be consumed mainly to form tetrahydrate; in that case, only a part of the energy would be consumed to distort the structural unit. Therefore, a great reduction in the content of strong acid may result. In addition, the formation of tetrahydrate would reduce the content of hexahydrate in the sample. That is, hexahydrate would be consumed and tetrahydrate and heptahydrate, both of which are considered to be ineffective for the appearance of strong acid, might be accumulated in the sample. These factors may also contribute to a reduction in the acidity of the lower H_0 values (strong acid).